On the dependence of QCD splitting functions on the choice of the evolution variable

S. Jadach,[a] A. Kusina,[b] W. Płaczek[c] and M. Skrzypek[a]

[a] *Institute of Nuclear Physics, Polish Academy of Sciences,*
 ul. Radzikowskiego 152, 31-342 Kraków, Poland
[b] *Laboratoire de Physique Subatomique et de Cosmologie,*
 53 Rue des Martyrs Grenoble, France
[c] *Marian Smoluchowski Institute of Physics, Jagiellonian University,*
 ul. Łojasiewicza 11, 30-348 Kraków, Poland

 E-mail: Stanislaw.Jadach@ifj.edu.pl, kusina@lpsc.in2p3.fr,
 wieslaw.placzek@uj.edu.pl, maciej.skrzypek@ifj.edu.pl

ABSTRACT: We show that already at the NLO level the DGLAP evolution kernel P_{qq} starts to depend on the choice of the evolution variable. We give an explicit example of such a variable, namely the maximum of transverse momenta of emitted partons and we identify a class of evolution variables that leave the NLO P_{qq} kernel unchanged with respect to the known standard $\overline{\text{MS}}$ results. The kernels are calculated using a modified Curci-Furmanski-Petronzio method which is based on a direct Feynman-graphs calculation.

Contents

1 Introduction

The choice of the evolution variable in the QCD evolution of the partonic densities is one of the key issues in the construction of any Monte Carlo parton shower [1]. The most popular choices are related to the virtuality, angle or transverse momentum of the emitted partons [2–4]. At the leading order (LO) level, commonly used for the simulations, the splitting functions are identical for all variables. In this note we investigate whether it is the case also beyond the LO. To calculate the evolution kernels we use slightly modified methodology of the Curci-Furmanski-Petronzio classical paper [5]. It is based on the direct calculation of the contributing Feynman graphs in the axial gauge, cf. [6]. The graphs are extracted by means of the projection operators which act by closing the fermionic or gluonic lines, putting the incoming partons on-shell and extracting pole parts of the expressions. The distinct feature of this approach is the fact that the singularities are regularized by means of the dimensional regularization, except for the "spurious" ones which are regulated by the principal value (PV) prescription. To this end, a dummy regulator δ is introduced with the help of the replacement

$$\frac{1}{ln} \rightarrow \frac{ln}{(ln)^2 + \delta^2(pn)^2}. \tag{1.1}$$
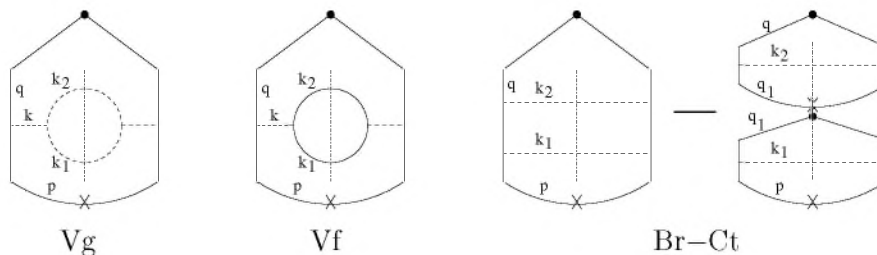
Figure 1. Real graphs with double poles contributing to the NLO non-singlet P_{qq} kernel. The solid lines represent quarks and the dotted lines stand for gluons.

The regulator δ is directly linked to the definition of the PV operation and has a simple geometrical cut-off-like interpretation. This way some of the poles in ϵ are replaced by the logarithms of δ. For more details we refer to the original paper [5] or to later calculations, for example [7–9]. The difference of our method with respect to the approach of [5] is the use of the New PV (NPV) prescription which we have introduced in [10, 11]. NPV amounts to the extension of the geometrical regularization to all singularities in the light cone l^+ variable, not only to the "spurious" ones. This modification turns out to be essential, as it further reduces the number of higher-order poles in ϵ by replacing them with the $\log \delta$ terms, and simplifies the contributions of the individual graphs.

There are three mechanisms which keep the kernel invariant under the change of the cut-off: (1) Invariance of a particular diagram. This applies to all diagrams with the single poles in ϵ. (2) Pairwise cancellation between the matching real and virtual graphs, as in Vg and Vf graphs of figure 1. (3) Cancellation between a graph and its counter-term. This is the case for ladder graphs. We will demonstrate that the mechanism (2) can fail already at the NLO level.

Our plan is the following. We will individually analyse the most singular diagrams contributing to the P_{qq} kernel. There are three graphs with second-order poles in ϵ contributing to the kernel; they are depicted in figure 1. We will calculate the difference between the kernel with the virtuality cut-off $-q^2 < Q^2$, as in the original paper [5], and with a set of different cut-offs. The cut-offs we consider are: the maximum and the scalar sum of the transverse momenta of the emitted partons, i.e. $\max\{k_{1\perp}, k_{2\perp}\}$ and $k_{1\perp} + k_{2\perp}$, as well as the maximum and the total rapidity of the emitted partons, i.e. $\max\{k_{1\perp}/\alpha_1, k_{2\perp}/\alpha_2\}$ and $|\vec{k}_{1\perp} + \vec{k}_{2\perp}|/(\alpha_1 + \alpha_2)$.[1] The calculation will show that three of these cut-offs leave the kernel unchanged with respect to the standard $\overline{\text{MS}}$ result, whereas, the one on the maximum of the transverse momenta leads to the change of the kernel. We will demonstrate in detail the mechanism of this change and we will formulate a general rule to identify cut-offs leading to it.

We will start with the diagram named Vg and its sibling Vf. Next, we will discuss the ladder graph Br and its counter term, Ct. Our analysis will demonstrate that only the Vg and Vf diagrams depend on the chosen cut-off variable. In the case of the ladder graph the counter term cancels the dependence. Finally, we will comment on why the graphs with

---

[1]We define $k_{i\perp} \equiv |\vec{k}_{i\perp}|$.
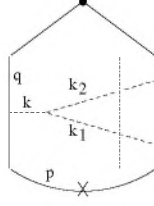
Figure 2. The graph Yg contributing to the NLO non-singlet P_{qq} kernel. The solid lines represent quarks and the dotted lines stand for gluons.

only single ϵ poles do not contribute. This is also the reason why NPV is instrumental: it replaces $1/\epsilon^3$ poles of the diagram Yg (depicted in figure 2) by the single poles and logarithms of the regulator δ. As a consequence, this diagram does not contribute in NPV, whereas it would have a nontrivial contribution in the original PV prescription.

2 Diagram Vg

In order to establish our notation and conventions, we give explicitly the starting formula for the contribution of the diagram Vg, corresponding to figure 1:

$$\Gamma_G = c_G^V g^4\, x\, \mathrm{PP}\left[\frac{1}{\mu^{4\epsilon}}\int d\Psi\delta\Big(x - \frac{qn}{pn}\Big)\frac{1}{q^4}W_G\right], \tag{2.1}$$

$$d\Psi = \frac{d^m k_1}{(2\pi)^m}2\pi\delta^+(k_1^2)\frac{d^m k_2}{(2\pi)^m}2\pi\delta^+(k_2^2) = (2\pi)^{-2m+2}\frac{1}{4}\frac{d\alpha_1}{\alpha_1}\frac{d\alpha_2}{\alpha_2}d^{m-2}\vec{k}_{1\perp}d^{m-2}\vec{k}_{2\perp}, \tag{2.2}$$

$$c_G^V = \frac{1}{2}C_G C_F, \tag{2.3}$$

$$W_G = \frac{1}{4qn}\frac{1}{k^4}\mathrm{Tr}\Big(\hat{n}\hat{q}\gamma^\mu\hat{p}\gamma^\lambda\hat{q}\Big)d_{\nu''\nu'}(k_2)d_{\mu\mu''}(k_1+k_2)d_{\lambda''\mu'}(k_1)d_{\mu'\lambda}(k_1+k_2)$$
$$\times\, V(k_1^{\mu''}+k_2^{\mu''},-k_2^{\nu''},-k_1^{\lambda''})V(k_1^{\mu'},k_2^{\nu'},-k_1^{\lambda'}-k_2^{\lambda'}). \tag{2.4}$$

We work in $m = 4 + 2\epsilon$ dimensions. The Sudakov variables are defined with the help of the light-like vector n and the initial-quark momentum p:

$$k_i = \alpha_i p + \alpha_i^- n + k_{i\perp}^{(m)}, \qquad q_i = x_i p + x_i^- n + q_{i\perp}^{(m)}, \tag{2.5}$$

$$p = (P, \vec{0}, P), \qquad n = \Big(\frac{pn}{2P}, \vec{0}, -\frac{pn}{2P}\Big). \tag{2.6}$$

Note that the vector symbol $\vec{}$ denotes $(m-2)$-dimensional Euclidean vectors in the transverse plane. Let us introduce the new integration variables, $\vec{\kappa}_1$ and $\vec{\kappa}_2$, instead of $\vec{k}_{1\perp}$ and $\vec{k}_{2\perp}$:

$$\vec{k}_{1\perp} = \vec{\kappa}_1 - \vec{\kappa}_2, \qquad \vec{k}_{2\perp} = \frac{\alpha_2}{\alpha_1}\vec{\kappa}_1 + \vec{\kappa}_2, \tag{2.7}$$

$$\text{i.e.} \quad \vec{\kappa}_1 = \frac{\alpha_1}{\alpha_1 + \alpha_2}\Big(\vec{k}_{1\perp} + \vec{k}_{2\perp}\Big), \quad \vec{\kappa}_2 = \frac{\alpha_1\alpha_2}{\alpha_1 + \alpha_2}\left(\frac{\vec{k}_{2\perp}}{\alpha_2} - \frac{\vec{k}_{1\perp}}{\alpha_1}\right), \tag{2.8}$$

$$\frac{\partial \vec{k}_{1\perp} \vec{k}_{2\perp}}{\partial \vec{\kappa}_1 \vec{\kappa}_2} = \left(\frac{1-x}{\alpha_1}\right)^{m-2}, \tag{2.9}$$

$$d\Psi = (2\pi)^{-2m+2} \frac{1}{4} \frac{d\alpha_1}{\alpha_1} \frac{d\alpha_2}{\alpha_2} \left(\frac{1-x}{\alpha_1}\right)^{m-2} \frac{1}{4} d\kappa_1^2 d\kappa_2^2 d\Omega_{m-3}^{(1)} d\Omega_{m-3}^{(2)} \kappa_1^{m-4} \kappa_2^{m-4}. \tag{2.10}$$

The benefit of these variables is the diagonal form of the variables k^2 and q^2 in which our formula is singular:

$$k^2 = \frac{(1-x)^2}{\alpha_1 \alpha_2} \kappa_2^2, \quad -q^2 = \frac{1-x}{\alpha_1}\left(\kappa_1^2 \frac{1}{\alpha_1} + \kappa_2^2 \frac{x}{\alpha_2}\right). \tag{2.11}$$

The trace W_G is of the form (θ is the angle between $\vec{\kappa}_1$ and $\vec{\kappa}_2$)

$$W_G = \frac{8}{x(1-x)^2}\left(\frac{\kappa_1^2}{\kappa_2^2} T_{Gc2} \cos^2\theta + \sqrt{\frac{\kappa_1^2}{\kappa_2^2}} T_{Gc} \cos\theta + \frac{\kappa_1^2}{\kappa_2^2} T_{GK} + T_{Gn}\right), \tag{2.12}$$

$$T_{Gc2} = 4(1+\epsilon)\frac{x\alpha_2^2}{(1-x)^2}, \tag{2.13}$$

$$T_{Gc} = x(1+x)\left((1+\epsilon)2(\alpha_1 - \alpha_2)\frac{\alpha_2}{(1-x)^2} + \frac{\alpha_2 - \alpha_1}{\alpha_1}\right), \tag{2.14}$$

$$T_{GK} = \frac{\alpha_1^2 + \alpha_2^2}{\alpha_1^2}\left(1 + x^2 + \epsilon(1-x)^2\right) + \alpha_2^2(1+\epsilon), \tag{2.15}$$

$$T_{Gn} = (1+\epsilon)\frac{x^2}{(1-x)^2}(\alpha_1 - \alpha_2)^2. \tag{2.16}$$

This allows us to rewrite formula (2.1) as

$$\Gamma_G = c_G^V g^4\, x\, \mathrm{PP}\Bigg[\frac{1}{\mu^{4\epsilon}} \int (2\pi)^{-2m+2} \frac{1}{4} \frac{d\alpha_1}{\alpha_1} \frac{d\alpha_2}{\alpha_2}\left(\frac{1-x}{\alpha_1}\right)^{m-2} \tag{2.17}$$

$$\times \frac{1}{4} d\kappa_1^2 d\kappa_2^2 d\Omega_{m-3}^{(1)} d\Omega_{m-3}^{(2)} \kappa_1^{m-4} \kappa_2^{m-4} \delta_{1-x-\alpha_1-\alpha_2}$$

$$\times \frac{1}{q^4} \frac{8}{x(1-x)^2}\left(\frac{\kappa_1^2}{\kappa_2^2} T_{Gc2} \cos^2\theta + \sqrt{\frac{\kappa_1^2}{\kappa_2^2}} T_{Gc} \cos\theta + \frac{\kappa_1^2}{\kappa_2^2} T_{GK} + T_{Gn}\right)\Bigg].$$

2.1 Cut-off on $\max\{k_{1\perp}, k_{2\perp}\} < Q$

Let us now perform the calculation of the Vg graph with the cut-off on the transverse momentum: $\max\{k_{1\perp}, k_{2\perp}\} < Q$. This diagram has two ϵ-type singularities, related to $1/q^2$ and $1/\kappa_2^2 \sim 1/k^2$. The kernel is constructed from the single-pole part of the diagram. Therefore, if we were able to separate the part of the diagram containing a double pole, we could considerably easier calculate the remaining single-pole part. This can be done if we calculate the difference between $\max\{k_{1\perp}, k_{2\perp}\} < Q$ and the standard virtuality-based cut-off $-q^2 < Q^2$. This way we exclude the region of the double ϵ pole. In the leftover difference the $d\kappa_2^2$ integral has to generate the single pole in ϵ and we can discard all terms finite in ϵ.

We now compute

$$\Delta\Gamma_{Vg}^{k_\perp - q} = \Gamma_G\left(\max\{k_{1\perp}, k_{2\perp}\} < Q\right) - \Gamma_G(-q^2 < Q^2). \tag{2.18}$$

The $-q^2 > Q^2$ translates into (see eq. (2.11))

$$-q^2 = c_1^2\kappa_1^2 + c_2^2\kappa_2^2 > Q^2 \Rightarrow \int_0 d\kappa_2^2(\kappa_2^2)^{-1+\epsilon} \int\limits_{(1/c_1)^2 Q^2 - (c_2/c_1)^2\kappa_2^2} d\kappa_1^2 \frac{(\kappa_1^2)^{1+\epsilon}}{(c_1^2\kappa_1^2 + c_2^2\kappa_2^2)^2}, \tag{2.19}$$

$$c_1^2 = \frac{1-x}{\alpha_1^2}, \quad c_2^2 = \frac{(1-x)x}{\alpha_1\alpha_2}. \tag{2.20}$$

In eq. (2.19) we have shown only the singular parts of the integrand. The singularities of the integral are located at $k^2 = \frac{(1-x)^2}{\alpha_1\alpha_2}\kappa_2^2 = 0$, i.e. at $\kappa_2 = 0$ and at $-q^2 = c_1^2\kappa_1^2 + c_2^2\kappa_2^2 = 0$ i.e. at $\kappa_1 = \kappa_2 = 0$. As we can see from (2.19), the $q^2 = 0$ area is excluded due to the subtraction of the $\Gamma_G(-q^2 < Q^2)$ which is available in the literature [5, 8]. The external integrals over $d\alpha$ cannot contribute additional $1/\epsilon$ poles as they are regulated by the NPV prescription. This is one of the two key ingredients of the calculation. Since we are interested in the pole part of $\Delta\Gamma$, we can expand the $d\kappa_2$ integrand in a standard way:

$$d\kappa_2^2(\kappa_2^2)^{-1+\epsilon} = d\kappa_2^2 \frac{1}{\epsilon}\delta_{\kappa_2^2=0} + \mathcal{O}(\epsilon^0). \tag{2.21}$$

This allows us to set κ_2 to zero in the rest of the formula (2.17), both in the integrand and in the integration limits. Furthermore, we can drop the terms T_{Gc} and T_{Gn} which do not have singularities in κ_2^2. Finally, we can set ϵ to zero in the remaining part of the formula. Altogether we obtain

$$\Delta\Gamma_{Vg}^{k_\perp - q} = c_G^V g^4 \, x(2\pi)^{-6} \frac{1}{2}\frac{1}{\epsilon}\frac{1}{x} \, \mathrm{PP}\Bigg[\int \frac{d\alpha_1}{\alpha_1^3}\frac{d\alpha_2}{\alpha_2}\frac{1}{c_1^4}\delta_{1-x-\alpha_1-\alpha_2} \tag{2.22}$$

$$\times \int\limits_{(1/c_1)^2 Q^2} \frac{d\kappa_1^2}{\kappa_1^2} \int d\Omega_1^{(1)} d\Omega_1^{(2)} \left(T_{Gc2}\cos^2\theta + T_{GK}\right)\Bigg].$$

Next, we have to fix the upper limit of the $d\kappa_1$ integral. We have

$$\max\{k_{1\perp}, k_{2\perp}\} < Q$$

$$\Rightarrow \max\left\{|\vec{\kappa}_1 - \vec{\kappa}_2|, \left|\frac{\alpha_2}{\alpha_1}\vec{\kappa}_1 + \vec{\kappa}_2\right|\right\} < Q$$

$$\Rightarrow |\vec{\kappa}_1 - \vec{\kappa}_2| < Q, \quad \left|\frac{\alpha_2}{\alpha_1}\vec{\kappa}_1 + \vec{\kappa}_2\right| < Q. \tag{2.23}$$

We are interested in the limits for κ_1 at the point $\kappa_2 = 0$. Immediately from eq. (2.23) we find

$$\kappa_1 < Q, \quad \frac{\alpha_2}{\alpha_1}\kappa_1 < Q. \tag{2.24}$$

Comments are in order regarding the integration limits for both of the angular integrals. One of the angles is trivial and covers the entire range $(0, 2\pi)$, as the system has rotational symmetry. The other angle, θ, between $\vec{\kappa}_1$ and $\vec{\kappa}_2$, has a non-trivial integration range, which depends on the kappas and alphas. However, there is a subspace where this angle is also unlimited. It is given by the conditions

$$\kappa_1 + \kappa_2 < Q, \quad \frac{\alpha_2}{\alpha_1}\kappa_1 + \kappa_2 < Q. \tag{2.25}$$

It just happens that in the limit $\kappa_2 = 0$ eq. (2.25) coincides with the entire range of κ_1. This way we find ($c_0 = \alpha_2/\alpha_1$)

$$\int_{(1/c_1)^2 Q^2}^{\min\{Q^2/c_0^2, Q^2\}} \frac{d\kappa_1^2}{\kappa_1^2} \int_0^{2\pi} d\Omega_1^{(1)} \int_0^{2\pi} d\theta \left(T_{Gc2}\cos^2\theta + T_{GK}\right) \tag{2.26}$$

$$= \left(\theta_{c_0<1}\ln c_1^2 + \theta_{c_0>1}\ln \frac{c_1^2}{c_0^2}\right) 2\pi \left(\pi T_{Gc2} + 2\pi T_{GK}\right)$$

$$= \left(\theta_{\alpha_2<\alpha_1}\ln \frac{1-x}{\alpha_1^2} + \theta_{\alpha_2>\alpha_1}\ln \frac{1-x}{\alpha_2^2}\right) 4\pi^2 \frac{\alpha_2}{\alpha_1 x} T_S,$$

$$T_S = x(1+x^2)\left(\frac{1}{(1-x)^2}\alpha_1\alpha_2 + \frac{\alpha_1^2 + \alpha_2^2}{\alpha_1\alpha_2}\right). \tag{2.27}$$

Going back to eq. (2.22) we obtain

$$\Delta\Gamma_{Vg}^{k_\perp - q} = c_G^V \frac{g^4}{(2\pi)^4}\frac{1}{2\epsilon}\frac{1}{x(1-x)^2} \int d\alpha_1 d\alpha_2 \delta_{1-x-\alpha_1-\alpha_2}\left(\ln(1-x) - 4\theta_{\alpha_2<\alpha_1}\ln\alpha_1\right)T_S. \tag{2.28}$$

Performing the α-integrals we find

$$\Delta\Gamma_{Vg}^{k_\perp - q} = c_G^V \left(\frac{\alpha_S}{\pi}\right)^2 \frac{1}{2\epsilon}\frac{1+x^2}{1-x}\left[\ln\frac{1}{(1-x)}\left(2I_0 + 2\ln(1-x) - \frac{11}{6}\right) - 4\left(\frac{11}{12}\ln 2 + \frac{131}{144} - \frac{\pi^2}{12}\right)\right], \tag{2.29}$$

where the symbol I_0 denotes the IR-divergent integral regularized by means of the PV prescription with the geometrical δ parameter:

$$I_0 = \int_0^1 d\alpha \frac{\alpha}{\alpha^2 + \delta^2} = -\frac{1}{2}\ln\delta^2, \tag{2.30}$$

$$I_1 = \int_0^1 d\alpha \ln\alpha \frac{\alpha}{\alpha^2 + \delta^2} = -\frac{1}{8}\ln^2\delta^2 - \frac{\pi^2}{24}. \tag{2.31}$$

The result (2.29) differs from the shift in virtual corrections shown later in section 4. We have obtained a net change of the kernel.

2.2 Cut-off on $k_{1\perp} + k_{2\perp} < Q$

We have demonstrated in the previous section that the change of real and virtual Vg-type diagrams do not compensate each other. Let's consider the virtual correction Vg, figure 3.
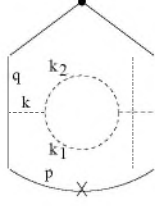
Figure 3. Real-virtual graph Vg contributing to NLO non-singlet P_{qq} kernel. The solid lines represent quarks and the dotted lines stand for gluons.

The graph has one real gluon, labelled k, and the cut-off is unique and trivial: $k_\perp \leq Q$. However, if we look inside the graph we find two virtual momenta, k_1 and k_2, such that $k_1 + k_2 = k$. Therefore, our $k_\perp$-cut-off at the unintegrated level is $|\vec{k}_{1\perp} + \vec{k}_{2\perp}| \leq Q$. This cut-off can be problematic for the real gluons because it does not close the phase space. We will get back to this issue in the next paragraph. For now, let us note that, as argued in section 2.1, we calculate only the difference between the q^2 and $k_\perp$ cut-offs. Therefore, we integrate only over the region singular in κ_2, i.e. we expand the $d\kappa_2$ integral according to eq. (2.21). This introduces $\kappa_2^2 = [\alpha_1\alpha_2/(1-x)^2]k^2 = 0$, or, equivalently, $\vec{k}_{1\perp}/\alpha_1 - \vec{k}_{2\perp}/\alpha_2 = 0$. In this subspace the condition $|\vec{k}_{1\perp} + \vec{k}_{2\perp}| \leq Q$ simplifies to $\kappa_1^2 \leq [\alpha_1/(1-x)]^2 Q^2 = [1/(1+c_0)]^2 Q^2$. In analogy, the "scalar" condition $|\vec{k}_{1\perp}| + |\vec{k}_{2\perp}| \leq Q$ simplifies to $|\vec{\kappa}_1| + |\vec{\kappa}_1|(\alpha_2/\alpha_1) \leq Q$, i.e. $\kappa_1^2 \leq [\alpha_1/(1-x)]^2 Q^2$, identical to the previous cut-off. Therefore, we expect that the "scalar" cut-off $|\vec{k}_{1\perp}| + |\vec{k}_{2\perp}| \leq Q$ will give the result compatible with the virtual correction. With this cut-off eq. (2.26) becomes

$$
\int\limits_{(1/c_1)^2 Q^2}^{[1/(1+c_0)]^2 Q^2} \frac{d\kappa_1^2}{\kappa_1^2} \int\limits_0^{2\pi} d\Omega_1^{(1)} \int\limits_0^{2\pi} d\theta \big(T_{Gc2}\cos^2\theta + T_{GK} \big) \tag{2.32}
$$

$$
= \ln\frac{c_1^2}{(1+c_0)^2} 2\pi \big(\pi T_{Gc2} + 2\pi T_{GK} \big)
$$

$$
= \ln\frac{1}{1-x} 4\pi^2 \frac{\alpha_2}{\alpha_1 x} T_S.
$$

Consequently, eq. (2.28) becomes

$$
\Delta\Gamma_{Vg}^{\Sigma k_\perp - q} = c_G^V \frac{g^4}{(2\pi)^4} \frac{1}{2\epsilon} \frac{1}{x(1-x)^2} \int d\alpha_1 d\alpha_2 \delta_{1-x-\alpha_1-\alpha_2} \ln\frac{1}{1-x} T_S \tag{2.33}
$$

$$
= c_G^V \Big(\frac{\alpha_S}{\pi}\Big)^2 \frac{1}{2\epsilon} \frac{1+x^2}{1-x} \ln\frac{1}{1-x} \Big(2I_0 + 2\ln(1-x) - \frac{11}{6} \Big). \tag{2.34}
$$

This way we reproduced result (2.29), but without the additional constant terms. It is identical to the change in the virtual corrections and there is no modification of the kernel.

2.3 Cut-off on $|\vec{k}_{1\perp} + \vec{k}_{2\perp}| \leq Q$

Let us come back to the cut-off on the vector variable $|\vec{k}_{1\perp} + \vec{k}_{2\perp}| \leq Q$. It indeed allows for the arbitrarily big values of $|\vec{k}_{i\perp}|$. The question is however whether it leads to well-defined and meaningful kernels? We will argue that it does.

Translated into the κ-variables of eq. (2.8), the cut-off is simply $\kappa_1 \leq \alpha_1/(1-x)Q$, identical to the one of section 2.2. The $\vec{\kappa}_2 = \vec{\kappa}_1 - \vec{k}_{1\perp}$ variable is unbounded because so is $\vec{k}_{1\perp}$ (the $\vec{k}_{2\perp}$ can always be adjusted to fulfill the cut-off) and the angle is also unlimited, $0 \leq \theta \leq 2\pi$. Keeping in mind the discussion on the origin of the poles given around eq. (2.21), we conclude that the upper limit on κ_2 does not matter at all, and we can set it to infinity as well. Repeating all the steps of section 2.2 we recover the result (2.34). In other words, we have just shown that the cut-off $|\vec{k}_{1\perp} + \vec{k}_{2\perp}| \leq Q$ leads to a proper kernel.

One may be worried weather the higher order terms of the ϵ-expansion of eq. (2.21) are finite. To answer this question let us inspect the original equations (2.1) and (2.12). In the limit $\kappa_2^2 \to \infty$ we have $-q^2 \sim (1-x)x/(\alpha_1\alpha_2)\kappa_2^2$ and we find the integrals of the type

$$\int\limits^{\infty} d\kappa_2^2 \left\{ \frac{1}{(\kappa_2^2)^3}, \frac{1}{(\kappa_2^2)^{5/2}}, \frac{1}{(\kappa_2^2)^2} \right\}, \tag{2.35}$$

which are integrable at the infinity. We conclude that the ϵ expansion of eq. (2.21) is legitimate and the cut-off $|\vec{k}_{1\perp} + \vec{k}_{2\perp}| \leq Q$ is self consistent. The open question is though how will this cut-off perform with other graphs. Another question concerns its generalization to more than two real partons.

2.4 Cut-off on rapidity

Let us briefly comment on the cut-off on rapidity. By rapidity we understand the quantity $a = |\vec{k}_\perp|/\alpha$ (massless) or $a = \sqrt{|\vec{k}_\perp|^2 + k^2}/\alpha$ (massive). For the case of two emissions the analogy to virtual graph leads to $a = |\vec{k}_{1\perp} + \vec{k}_{2\perp}|/(\alpha_1 + \alpha_2) \leq Q$ or $a = \sqrt{|\vec{k}_{1\perp} + \vec{k}_{2\perp}|^2 + (k_1 + k_2)^2}/(\alpha_1 + \alpha_2) \leq Q$. In the subspace $\kappa_2^2 \sim k^2 = 0$ both formulas coincide and both are identical to the $k_\perp$-type formula with the cut-off Q shifted to $Q(1-x)$ in the $k_\perp$-type formula. This is just the result we have obtained for the virtual corrections. Another option is $\max\{a_1, a_2\} \leq Q$. One has $\vec{a}_1 = (\vec{\kappa}_1 - \vec{\kappa}_2)/\alpha_1$ and $\vec{a}_2 = \vec{\kappa}_1/\alpha_1 + \vec{\kappa}_2/\alpha_2$. At $\kappa_2 = 0$ this leads to $\kappa_1/\alpha_1 \leq Q$ or equivalently $|\vec{k}_{1\perp} + \vec{k}_{2\perp}|/(\alpha_1 + \alpha_2) \leq Q$. This is identical to the previous case, so we expect the result to be in agreement with the virtual correction as well.

Let us compute the correction from the q^2-type to a-type cut-off. To this end, we generalize eq. (2.26), which is the $k_\perp$-type, by replacing $Q^2 \to Q^2(1-x)^\sigma$ in the upper limit: $\sigma = 2$ corresponds to the rapidity case discussed here, $\sigma = 0$ is the $k_\perp$ case (reference) and $\sigma = 1$ is the virtuality case (the correction vanishes). This is so because: $\Sigma k_\perp = ((1-x)/\alpha_1)^2\kappa_1^2 \leq Q^2$ is described by eq. (2.26). $a = k_\perp/(1-x) \to \kappa_1/\alpha_1 \leq Q$ requires multiplication of Q^2 by $(1-x)^2$ (with respect to the $k_\perp$ case). $-q^2 \to (1-x)\kappa_1^2/\alpha_1^2 \leq Q^2$ requires multiplication of Q^2 by $1-x$.

$$\int\limits_{(1/c_1)^2 Q^2}^{[(1-x)^\sigma/(1+c_0)]^2 Q^2} \frac{d\kappa_1^2}{\kappa_1^2} \int\limits_0^{2\pi} d\Omega_1^{(1)} \int\limits_0^{2\pi} d\theta \left(T_{Gc2} \cos^2\theta + T_{GK} \right) \tag{2.36}$$

$$= \ln\frac{c_1^2(1-x)^\sigma}{(1+c_0)^2} 2\pi \left(\pi T_{Gc2} + 2\pi T_{GK} \right)$$

$$= \ln(1-x)^{\sigma-1} 4\pi^2 \frac{\alpha_2}{\alpha_1 x} T_S.$$
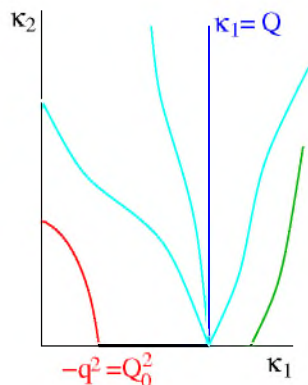
Figure 4. The (κ_1, κ_2) plane. The cut-off $\kappa_1 \leq Q$ is shown in dark blue. A family of other cut-off lines is shown in light blue. At the bottom left the $-q^2 \leq Q_0^2$ line is plotted in red. The singularities lie at the origin of the frame $(q^2 = 0)$ and along the line $\kappa_2^2 \sim k^2 = 0$. The integration path is the thick black line along $\kappa_2 = 0$ between the crossing points of $-q^2 = Q_0^2$ and the cut-off with the axis.

Consequently, eq. (2.28) becomes

$$
\begin{aligned}
\Delta\Gamma_{Vg}^{\sigma-q} &= c_G^V \frac{g^4}{(2\pi)^4} \frac{1}{2\epsilon} \frac{1}{x(1-x)^2} \int d\alpha_1 d\alpha_2 \delta_{1-x-\alpha_1-\alpha_2} \ln(1-x)^{\sigma-1} T_S \\
&= c_G^V \left(\frac{\alpha_S}{\pi}\right)^2 \frac{1}{2\epsilon} \frac{1+x^2}{1-x} \ln(1-x)^{\sigma-1} \left(2I_0 + 2\ln(1-x) - \frac{11}{6}\right).
\end{aligned}
\tag{2.37}
$$

2.5 General rule

We can now generalize the analysis of the previous sections and formulate a more universal rule for identifying the variables that do or do not change the NLO kernel.

In figure 4 we show the (κ_1, κ_2) plane. The blue cut-off $\vec{\kappa}_1 \leq Q$ is shown along with a family of other cut-off lines. Some of them (blue) are equivalent if they cross the κ_1-axis at the same point. The cut-offs may close the κ_2-direction from above or leave it open. At the bottom left we plot the red $-q^2 \leq Q_0^2$ line. The singularities lie at the origin of the frame $(q^2 = 0)$ and along the line $\kappa_2^2 \sim k^2 = 0$. The integration path is the thick line along $\kappa_2 = 0$ between crossing points of $-q^2 = Q_0^2$ and the cut-off with the axis.

The strategy we use is the following. We take a group of variables that coincide at the LO level (i.e. for single emission), we express them in terms of the variables κ and set $\kappa_2 = 0$. All the variables that cross the κ_1 axis at the same point will lead to the same result. It is now a matter of choosing one of them, calculating the shift as outlined, and comparing it with the shift in the virtual corrections. We collect the shifts in the virtual corrections for the basic three types of variables in section 4.

3 Diagram Vf

Let us now perform the analysis of the Vf graph. It will heavily rely on the analysis done for the Vg graph. Let us begin with the $\max\{k_{1\perp}, k_{2\perp}\}$ calculation. Our starting point is

the diagram depicted in figure 1. The analytical formula is analogous to eq. (2.1):

$$\Gamma_F = c_F^V g^4 \, x \, \text{PP} \left[\frac{1}{\mu^{4\epsilon}} \int d\Psi \delta \left(x - \frac{qn}{pn} \right) \frac{1}{q^4} W_F \right], \tag{3.1}$$

$$c_F^V = C_F T_F, \tag{3.2}$$

$$W_F = \frac{1}{4qn} \frac{1}{k^4} \text{Tr} \left(\hat{n} \hat{q} \gamma^\mu \hat{p} \gamma^\lambda \hat{q} \right) d_{\mu\mu''} (k_1 + k_2) \text{Tr} \left(\hat{k}_2 \gamma^{\mu''} \hat{k}_1 \gamma^{\mu'} \right) d_{\mu'\lambda} (k_1 + k_2)$$

$$= \frac{32pn}{4qn} \frac{1}{(1-x)^2} \left(\frac{\kappa_1^2}{\kappa_2^2} T_{Fc2} \cos^2 \theta + \sqrt{\frac{\kappa_1^2}{\kappa_2^2}} T_{Fc} \cos \theta + \frac{\kappa_1^2}{\kappa_2^2} T_{FK} + T_{Fn} \right), \tag{3.3}$$

$$T_{Fc2} = -4x \frac{\alpha_2^2}{v^2}, \tag{3.4}$$

$$T_{Fc} = 2x (1 + x) \alpha_2 (\alpha_2 - \alpha_1) \frac{1}{v^2}, \tag{3.5}$$

$$T_{FK} = \frac{1}{2} \epsilon v^2 \frac{\alpha_2}{\alpha_1} + \frac{1}{2} (1 + x^2) \frac{\alpha_2}{\alpha_1} - \alpha_2^2, \tag{3.6}$$

$$T_{Fn} = 4 \frac{x^2}{v^2} \alpha_1 \alpha_2. \tag{3.7}$$

The calculation goes now in a complete analogy to the Vg case and we arrive at the adapted version of eq. (2.28) into which we plug in the expression for the $T_S^{(F)}$ function

$$\Delta\Gamma_{Vf}^{k_\perp - q} = c_F^V \frac{g^4}{(2\pi)^4} \frac{1}{2\epsilon} \frac{1}{x(1-x)^2} \int d\alpha_1 d\alpha_2 \delta_{1-x-\alpha_1-\alpha_2} \left(\ln(1-x) - 4\theta_{\alpha_2 < \alpha_1} \ln \alpha_1 \right) T_S^{(F)}, \tag{3.8}$$

$$T_S^{(F)} = \frac{\alpha_1}{\alpha_2} x \left(\frac{1}{2} T_{Fc2}^{(0)} + T_{FK}^{(0)} \right) = \frac{1}{2} x(1 + x^2) \left(-2 \frac{1}{(1-x)^2} \alpha_1 \alpha_2 + 1 \right). \tag{3.9}$$

Once the $d\alpha$-integration is done we obtain the final result for the Vf graph with the cut-off on $\max k_\perp$

$$\Delta\Gamma_{Vf}^{k_\perp - q} = c_F^V \left(\frac{\alpha}{2\pi} \right)^2 \frac{2}{\epsilon} \frac{1 + x^2}{1 - x} \left[-\frac{1}{3} \ln(1 - x) + \frac{23}{36} - \frac{2}{3} \ln 2 \right]. \tag{3.10}$$

Let us discuss also the other choices of the cut-offs: the sum of $k_\perp$, virtuality and rapidity, labelled as $\sigma = 0, 1, 2$, respectively. For this purpose it is enough to repeat the analysis and reuse the formulas for the Vg graph. The formula (2.37) can be directly used to give

$$\Delta\Gamma_{Vf}^{\sigma - q} = c_F^V \frac{g^4}{(2\pi)^4} \frac{1}{2\epsilon} \frac{1}{x(1-x)^2} \int d\alpha_1 d\alpha_2 \delta_{1-x-\alpha_1-\alpha_2} \ln (1 - x)^{\sigma - 1} T_S^{(F)}$$

$$= c_F^V \left(\frac{\alpha_S}{2\pi} \right)^2 \frac{2}{\epsilon} \frac{1 + x^2}{1 - x} \frac{1}{3} \ln (1 - x)^{\sigma - 1}. \tag{3.11}$$

$$\Delta\Gamma_{Vf}^{\Sigma k_\perp - q} = c_F^V \left(\frac{\alpha}{2\pi} \right)^2 \frac{2}{\epsilon} \frac{1 + x^2}{1 - x} \left[-\frac{1}{3} \ln(1 - x) \right], \tag{3.12}$$

$$\Delta\Gamma_{Vf}^{a - q} = c_F^V \left(\frac{\alpha}{2\pi} \right)^2 \frac{2}{\epsilon} \frac{1 + x^2}{1 - x} \left[\frac{1}{3} \ln(1 - x) \right]. \tag{3.13}$$

4 Virtual diagrams

The shift in the virtual corrections due to the change of the cut-off can be found in ref. [9]. The σ-dependence of each diagram is given there. One finds that there is no σ-dependence for the C_F^2-type graphs and the only ones that do depend on σ are Vg and Vf, see eqs. (4.25) and (4.31) in ref. [9]. Here we quote the change with respect to the virtuality case:

$$\Delta\Gamma_{virt}^{\sigma-q} = \left(\frac{\alpha}{2\pi}\right)^2 \frac{1}{2\epsilon} C_F \frac{1+x^2}{1-x}\Big(\beta_0 - 4C_A\big(I_0 + \ln(1-x)\big)\Big) \ln^{\sigma-1}(1-x). \qquad (4.1)$$

5 Combined Vg+Vf real diagrams

Let us combine the Vg and Vf real graphs for the case of $\max\{k_{1\perp}, k_{2\perp}\}$. The formulas to be added are (2.29) and (3.10) with $c_G^V = (1/2)C_F C_A$ and $c_F^V = C_F T_F$:

$$\Delta\Gamma_{Vf+Vg}^{k_\perp-q} = C_F\left(\frac{\alpha_S}{2\pi}\right)^2 \frac{2}{\epsilon}\frac{1+x^2}{1-x}\left[-C_A\Big(I_0 + \ln(1-x)\Big)\ln(1-x)\right.$$
$$\left. + C_A\frac{\pi^2}{6} - C_A\frac{1}{16} + \frac{1}{4}\beta_0\ln(1-x) + \frac{1}{2}\beta_0\ln 2 - \frac{23}{48}\beta_0\right], \qquad (5.1)$$

$$\beta_0 = \frac{11}{3}C_A - \frac{4}{3}T_F. \qquad (5.2)$$

Anticipating the results of the following sections we can state that this result represents the change of the P_{qq} kernel due to the real corrections when the evolution variable (cut-off) is changed from the standard q^2 one to the $\max\{k_{1\perp}, k_{2\perp}\}$. Supplied with the virtual corrections it will give the complete effect.

Let us combine also the σ-type cut-offs for the real Vf+Vg graphs

$$\Delta\Gamma_{Vf+Vg}^{\sigma-q} = C_F\left(\frac{\alpha_S}{2\pi}\right)^2 \frac{1}{2\epsilon}\frac{1+x^2}{1-x}\ln(1-x)^{\sigma-1}\left[-\beta_0 + 4C_A\Big(I_0 + \ln(1-x)\Big)\right]. \qquad (5.3)$$

6 Added real and virtual diagrams

We can now add changes of the real and the virtual Vf+Vg graphs. For the σ-type cut-offs we observe that the contributions cancel each other and there is no net effect, as expected. The situation is different for the cut-off on $\max\{k_{1\perp}, k_{2\perp}\}$, where we find the following shift

$$\Delta\Gamma_{Vf+Vg,R+V}^{k_\perp-q} = C_F\left(\frac{\alpha_S}{2\pi}\right)^2 \frac{1}{2\epsilon}\frac{1+x^2}{1-x}\left[C_A\frac{2\pi^2}{3} - C_A\frac{1}{4} + 2\beta_0\ln 2 - \frac{23}{12}\beta_0\right]. \qquad (6.1)$$

This result can be translated into the kernel P_{qq} which is the residue of Γ [5]:

$$\Gamma = \delta_{1-x} + \frac{1}{\epsilon}\left[\left(\frac{\alpha}{2\pi}\right)P^{(1)} + \frac{1}{2}\left(\frac{\alpha}{2\pi}\right)^2 P^{(2)} + \dots\right], \qquad (6.2)$$

$$P_{qq} = \left(\frac{\alpha}{2\pi}\right)P^{(1)} + \left(\frac{\alpha}{2\pi}\right)^2 P^{(2)} + \dots, \qquad (6.3)$$

and we obtain the following change of the P_{qq} kernel

$$P_{qq}(\max\{k_{1\perp}, k_{2\perp}\} < Q) - P_{qq}(-q^2 < Q^2) =$$
$$= C_F \left(\frac{\alpha_S}{2\pi}\right)^2 \frac{1+x^2}{1-x}\left[C_A\left(\frac{2\pi^2}{3} - \frac{1}{4}\right) + \beta_0\left(2\ln 2 - \frac{23}{12}\right)\right]. \tag{6.4}$$

This is the central new result of this paper.

7 Br (ladder) graph and counter term

We now turn to the ladder graph and the counter term associated with it, shown in figure 1. Both of them have double ϵ poles and therefore can be modified once the evolution variable changes. However, we will demonstrate that their difference remains unchanged.

The contribution Γ_{Br} of the ladder graph is similar to the one given for the Vg graph in eqs. (2.1), (2.2)

$$\Gamma_{Br} = C_F^2 \frac{g^4\, x}{(2\pi)^6} \mathrm{PP}\left[\frac{(2\pi)^{-2\epsilon}}{\mu^{2\epsilon}} \int \frac{d\alpha_2}{2\alpha_2} d^{2+2\epsilon}\vec{k}_{2\perp} \frac{(2\pi)^{-2\epsilon}}{\mu^{2\epsilon}} \int \frac{d\alpha_1}{2\alpha_1} d^{2+2\epsilon}\vec{k}_{1\perp} \delta_{1-x-\alpha_1-\alpha_2} \frac{1}{q^4}\frac{1}{q_1^4} W_{Br}\right]. \tag{7.1}$$

$$W_{Br} = \frac{1}{4qn}\mathrm{Tr}\left(\hat{n}\hat{q}\hat{\gamma}^\mu \hat{q}_1\hat{\gamma}^\alpha \hat{p}\hat{\gamma}^\beta \hat{q}_1 \hat{\gamma}^\nu \hat{q}\right) d_{\alpha\beta}(k_1) d_{\mu\nu}(k_2). \tag{7.2}$$

$$= \frac{4}{x\alpha_1\alpha_2} \frac{k_{1\perp}^2}{\alpha_1}\left(\frac{k_{1\perp}^2}{\alpha_1} T_1 + \frac{k_{2\perp}^2}{\alpha_2} T_2 + 2\vec{k}_{1\perp}\cdot\vec{k}_{2\perp} T_3\right), \tag{7.3}$$

$$T_1 = (x^2 + x_1^2 + 1)(1-x_1)(x_1 - x) + \mathcal{O}(\epsilon), \tag{7.4}$$

$$T_2 = \left(1 + x_1^2 + \epsilon(1-x_1)^2\right)\left(x^2 + x_1^2 + \epsilon(x_1 - x)^2\right), \tag{7.5}$$

$$T_3 = x_1(x^2 + x_1^2 + 1) + \mathcal{O}(\epsilon), \tag{7.6}$$

$$q_1^2 = -\frac{k_{1\perp}^2}{\alpha_1} = -\frac{q_{1\perp}^2}{\alpha_1}. \tag{7.7}$$

As before, we will calculate only the difference w.r.t. the result with cut-off on the virtuality, $-q^2 < Q^2$. Therefore, the pole coming from the $1/q^2$ integrand is eliminated and we are forced to keep only terms that generate the ϵ pole from the $dk_{1\perp}^2$ integral. This means that we keep only T_2, set to zero all other ϵ-terms and expand $dk_{1\perp}^2$-integral, i.e.

$$T_1 = T_3 = 0,$$
$$\epsilon \to 0 \quad \text{except } k_{1\perp}^{2\epsilon}, \tag{7.8}$$
$$\int dk_{1\perp}^2 k_{1\perp}^{-2+2\epsilon} \to \frac{1}{\epsilon} \int \delta(k_{1\perp}^2) dk_{1\perp}^2.$$

This way we obtain

$$\Gamma_{Br}^{(q)} = C_F^2 \frac{g^4}{(2\pi)^6} 4\mathrm{PP}\left[\int\limits_{-q^2 > Q^2} \frac{d\alpha_2}{2\alpha_2^3} d^2\vec{k}_{2\perp} \int \frac{d\alpha_1}{2\alpha_1} d^{2+2\epsilon}\vec{k}_{1\perp} \delta_{1-x-\alpha_1-\alpha_2} \frac{k_{2\perp}^2}{q^4}\frac{1}{k_{1\perp}^2} T_2(\epsilon = 0)\right]. \tag{7.9}$$

The matching counter term Γ_{Br}^{Ct} differs only by the "split" of the trace W_{Br}^{ct} and an additional projection operator. The projection operator performs two actions: picks the ϵ-poles and sets on-shell the incoming quark (q_1 in our case). These are minor modifications to (7.1), (7.3):

$$\Gamma_{Br}^{Ct} = C_F^2 \frac{g^4}{(2\pi)^6} \frac{x}{(2\pi)^6} \mathrm{PP}\left[\frac{(2\pi)^{-2\epsilon}}{\mu^{2\epsilon}} \int_{-q^2>Q^2} \frac{d\alpha_2}{2\alpha_2} d^{2+2\epsilon}\vec{k}_{2\perp} \frac{1}{q^4} W_{Br2}\bigg|_{q_1^2=0} \right.$$

$$\left. \times \mathrm{PP}\left(\frac{(2\pi)^{-2\epsilon}}{\mu^{2\epsilon}} \int \frac{d\alpha_1}{2\alpha_1} d^{2+2\epsilon}\vec{k}_{1\perp} \frac{\alpha_1^2}{k_{1\perp}^4} W_{Br1} \delta_{1-x-\alpha_1-\alpha_2} \right) \right], \qquad (7.10)$$

where

$$W_{Br2} = \frac{1}{4qn}\mathrm{Tr}\left(\hat{n}\hat{q}\hat{\gamma}^\mu\hat{q}_1\hat{\gamma}^\nu\hat{q}\right)d_{\mu\nu}(k_2)\bigg|_{q_1^2=0} = -2q^2 \frac{1}{x\alpha_2}(x_1^2 + x^2 + \epsilon(x_1-x)^2), \qquad (7.11)$$

$$W_{Br1} = \frac{1}{4q_1 n}\mathrm{Tr}\left(\hat{n}\hat{q}_1\hat{\gamma}^\alpha\hat{p}\hat{\gamma}^\beta\hat{q}_1\right)d_{\alpha\beta}(k_1) = -2q_1^2 \frac{1}{x_1\alpha_1}(1 + x_1^2 + \epsilon(1-x_1)^2), \qquad (7.12)$$

and thanks to the condition $q_1^2 = 0$:

$$q_1^2 = -\frac{k_{1\perp}^2}{\alpha_1}, \quad q^2\bigg|_{q_1^2=0} = -x\left(\frac{k_{1\perp}^2}{\alpha_1} + \frac{k_{2\perp}^2}{\alpha_2}\right) - k_\perp^2\bigg|_{k_{1\perp}^2=0} = -\frac{x_1 k_{2\perp}^2}{\alpha_2}. \qquad (7.13)$$

We obtain

$$\Gamma_{Br}^{Ct} = C_F^2 \frac{g^4}{(2\pi)^6} 4\mathrm{PP}\left[\int_{-q^2>Q^2} \frac{d\alpha_2}{2\alpha_2^3} d^2\vec{k}_{2\perp} \frac{k_{2\perp}^2}{q^4}\bigg|_{q_1^2=0} \int \frac{d\alpha_1}{2\alpha_1} d^{2+2\epsilon}\vec{k}_{1\perp} \frac{1}{k_{1\perp}^2} \delta_{1-x-\alpha_1-\alpha_2} T_2(\epsilon=0) \right]. \qquad (7.14)$$

It is easy to verify now that these two quantities, Γ_{Br} and Γ_{Br}^{Ct}, are identical under the conditions (7.8) and the net change of the kernel is zero.

In appendix A we evaluate the change of the ladder graph alone caused by the change of the cut-off. This quantity is of interest, for example, in the construction of Monte Carlo algorithms.

8 Conclusions

In this paper we have discussed the change of the DGLAP kernel P_{qq} due to the change of the evolution variable within the CFP scheme. We have demonstrated that at the NLO level majority of the choices of the evolution variables lead to the same kernel, but there are ones, like the maximal transverse momentum, that correspond to the modified kernel. We have explained the mechanism responsible for the change and we have formulated a simple rule to identify classes of variables that leave the kernel unchanged at the NLO level.

There is an important open question related to our analysis: is the kernel dependence specific to the CFP method and specifically to the presence of the geometrical cut-off δ? If all the singularities, including the "spurious" ones, were regulated by the dimensional

regularization, the structure of the ϵ poles would be more complex, more graphs would have higher-order poles in ϵ and would contribute to the modification of the kernel. This would, however, be a surprising result showing that the choice of the seemingly dummy technical regulator has physical consequences. The same question holds for the modification of the original PV prescription of [5] to the NPV one used in this note.

Of course, this question can be addressed also from the perspective of different methods which employ calculation of the total cross sections for physical processes to obtain splitting functions. Such a viewpoint would allow us to interpret our result in terms of a finite scheme transformation. This however, goes beyond the scope of the current work and we leave it for a future study. Our current results are valid within the CFP method.

Acknowledgments

A Change of ladder graph with cut-off

In the appendix we calculate the change of the Γ_{Br} for various cut-offs as it can be useful in constructing Monte Carlo algorithms. Let us continue with eq. (7.1) and let us implement the conditions (7.8):

$$\int d^{2+2\epsilon}\vec{k}_{1\perp}\frac{1}{k_{1\perp}^2} = \int \frac{1}{2}\frac{dk_{1\perp}^2}{k_{1\perp}^2}k_{1\perp}^{2\epsilon}d\Omega_{1+\epsilon}^{(k_{1\perp})} \to \int \frac{1}{2}dk_{1\perp}^2\frac{1}{\epsilon}\delta(k_{1\perp}^2)d\Omega_1^{(k_{1\perp})} = 2\pi\frac{1}{2\epsilon} \quad (\text{A.1})$$

$$\int_L^U d^{2+2\epsilon}\vec{k}_{2\perp}\frac{1}{k_{2\perp}^2} \to \int_L^U \frac{1}{2}dk_{2\perp}^2 k_{2\perp}^{-2}d\Omega_1^{(k_{2\perp})} = \pi\ln\frac{U}{L}. \quad (\text{A.2})$$

The lower limit on the integral $d^{2+2\epsilon}\vec{k}_{2\perp}$ follows from the fact that we compute the difference w.r.t. the virtuality-based formula. This leads to the condition

$$Q^2 < -q^2 = \frac{x_1 k_{2\perp}^2}{\alpha_2} \to k_{2\perp}^2 > Q^2\frac{\alpha_2}{x_1}. \quad (\text{A.3})$$

The upper limit depends on the chosen evolution variable. We will examine a few cases. The cut-offs and their simplified versions once the condition (A.1), i.e. $k_{1\perp} = 0$, is applied are as follows:

$$\left.\begin{array}{ll}(A): & \max\{k_{1\perp}, k_{2\perp}\}\\ (B): & k_{1\perp} + k_{2\perp}\\ (C): & \max\{\frac{k_{1\perp}}{\alpha_1}, \frac{k_{2\perp}}{\alpha_2}\}\\ (D): & \frac{|\vec{k}_{1\perp}+\vec{k}_{2\perp}|}{\alpha_1+\alpha_2}\end{array}\right\} \overset{k_{1\perp}=0}{\Longrightarrow} \left\{\begin{array}{ll}(A): & k_{2\perp} < Q\\ (B): & k_{2\perp} < Q\\ (C): & k_{2\perp} < \alpha_2 Q\\ (D): & k_{2\perp} < (1-x)Q\end{array}\right. \quad (\text{A.4})$$

eq. (7.1) transforms now into

$$\Delta\Gamma_{Br}^{U-q^2} = C_F^2\left(\frac{\alpha}{2\pi}\right)^2\left[\int\frac{d\alpha_2}{\alpha_2}\ln\frac{U}{L}\int\frac{d\alpha_1}{\alpha_1}\frac{1}{2\epsilon}\delta_{1-x-\alpha_1-\alpha_2}\frac{1}{x_1^2}\left(1+x_1^2\right)\left(x^2+x_1^2\right)\right]. \quad (\text{A.5})$$

Let us continue with each case separately.

Cases (A) and (B): $\max\{k_{1\perp}, k_{2\perp}\}$ and $k_{1\perp} + k_{2\perp}$

$$\Gamma_{Br}^{k_\perp - q^2} = C_F^2 \left(\frac{\alpha}{2\pi}\right)^2 \frac{1}{2\epsilon} \int\limits_0^{1-x} \frac{d\alpha_1}{\alpha_1 \alpha_2} \frac{1}{x_1^2} \left(1 + x_1^2\right)\left(x^2 + x_1^2\right) \ln \frac{x_1}{\alpha_2} \tag{A.6}$$

$$= C_F^2 \left(\frac{\alpha}{2\pi}\right)^2 \frac{1}{2\epsilon} \frac{1}{1-x} \int\limits_0^{1-x} d\alpha_1 (U_0 + U_l + U_u),$$

$$U_0 = \left(\frac{1}{1-x_1} + \frac{1}{x_1 - x}\right) \frac{1}{x_1^2} \left(1 + x_1^2\right)\left(x^2 + x_1^2\right) \ln \frac{x_1}{x_1 - x} - U_l - U_u, \tag{A.7}$$

$$U_l = \frac{1}{1-x_1} 2(1 + x^2) \ln \frac{1}{1-x}, \tag{A.8}$$

$$U_u = \frac{1}{x_1 - x} 2(1 + x^2) \ln \frac{x}{x_1 - x}, \tag{A.9}$$

where we have subtracted and added the singular integrals of the $I_{0,1}$ type. The direct integration gives

$$\int\limits_0^{1-x} d\alpha_1 U_0 = -(1-x)^2 + (1+x^2)\ln^2 x + (1+3x^2)\frac{\pi^2}{6} + 2(1-x)^2 \ln(1-x)$$
$$- (x^2 - 1)\mathrm{Li}_2(x) + x(1-x)\ln x \tag{A.10}$$

$$\int\limits_0^{1-x} d\alpha_1 U_l = 2(1 + x^2)(I_0 + \ln(1-x)) \ln \frac{1}{1-x} \tag{A.11}$$

$$\int\limits_0^{1-x} d\alpha_1 U_u = 2(1 + x^2)(I_0 + \ln(1-x)) \ln x - 2(1 + x^2)\left(I_1 + \frac{1}{2}\ln^2(1-x)\right)$$
$$= 2(1 + x^2)\left(-I_1^{(1-x)} + I_0^{(1-x)} \ln \frac{x}{1-x}\right), \tag{A.12}$$

where

$$\begin{aligned} I_0^{(1-x)} &= I_0 + \ln(1-x), \\ I_1^{(1-x)} &= I_1 - I_0 \ln(1-x) + \frac{1}{2}\ln^2(1-x). \end{aligned} \tag{A.13}$$

Hence

$$\Gamma_{Br}^{k_\perp - q^2} = C_F^2 \left(\frac{\alpha}{2\pi}\right)^2 \frac{1}{2\epsilon}\left[-(1-x) - (1+x)\frac{\pi^2}{6} + 2(1-x)\ln(1-x) + (1+x)\mathrm{Li}_2(x)\right.$$
$$\left. + x\ln x + 2\frac{1+x^2}{1-x}\left(-I_1^{(1-x)} + I_0^{(1-x)} \ln \frac{x}{(1-x)^2} + \frac{1}{2}\ln^2 x + \frac{\pi^2}{6}\right)\right]. \tag{A.14}$$

Case (C): $\max\{\frac{k_{1\perp}}{\alpha_1}, \frac{k_{2\perp}}{\alpha_2}\}$

$$\Gamma_{Br}^{k_\perp/a - q^2} = C_F^2 \left(\frac{\alpha}{2\pi}\right)^2 \frac{1}{2\epsilon} \int\limits_0^{1-x} \frac{d\alpha_1}{\alpha_1 \alpha_2} \frac{1}{x_1^2} \left(1 + x_1^2\right)\left(x^2 + x_1^2\right) \ln(x_1 \alpha_2) \tag{A.15}$$

$$= C_F^2 \Big(\frac{\alpha}{2\pi}\Big)^2 \frac{1}{2\epsilon} \Bigg[1 - x + (1+x)\ln^2 x + (1+x)\frac{\pi^2}{6} - 2(1-x)\ln(1-x) - (2-x)\ln x$$

$$- (1+x)\mathrm{Li}_2(x) + 2\frac{1+x^2}{1-x}\Big(I_1^{(1-x)} + I_0^{(1-x)}\ln\big(x(1-x)^2\big) - \frac{\pi^2}{6} + \frac{1}{2}\ln^2 x \Big) \Bigg]. \quad \text{(A.16)}$$

Case (D): $|\vec{k}_{1\perp} + \vec{k}_{2\perp}|/(\alpha_1 + \alpha_2)$

$$\Gamma_{Br}^{k_\perp/(1-x)-q^2} = C_F^2 \Big(\frac{\alpha}{2\pi}\Big)^2 \frac{1}{2\epsilon} \int\limits_0^{1-x} \frac{d\alpha_1}{\alpha_1 \alpha_2} \frac{1}{x_1^2} \big(1 + x_1^2\big)\big(x^2 + x_1^2\big) \ln\frac{x_1(1-x)}{\alpha_2}$$

$$= C_F^2 \Big(\frac{\alpha}{2\pi}\Big)^2 \frac{1}{2\epsilon} \Bigg[-(1-x) - (1+x)\mathrm{Li}_2(1-x) + x\ln x$$

$$2\frac{1+x^2}{1-x}\Big(-I_1^{(1-x)} + I_0^{(1-x)}\ln x + \frac{\pi^2}{6} + \frac{1}{2}\ln^2 x \Big) \Bigg]. \quad \text{(A.17)}$$

Open Access. This article is distributed under the terms of the Creative Commons Attribution License (CC-BY 4.0), which permits any use, distribution and reproduction in any medium, provided the original author(s) and source are credited.

References

[1] M. Bengtsson and T. Sjöstrand, *A Comparative Study of Coherent and Noncoherent Parton Shower Evolution*, *Nucl. Phys.* **B 289** (1987) 810 [INSPIRE].

[2] T. Sjöstrand, *A Model for Initial State Parton Showers*, *Phys. Lett.* **B 157** (1985) 321 [INSPIRE].

[3] T. Sjöstrand and P.Z. Skands, *Transverse-momentum-ordered showers and interleaved multiple interactions*, *Eur. Phys. J.* **C 39** (2005) 129 [hep-ph/0408302] [INSPIRE].

[4] M. Bahr et al., *HERWIG++ Physics and Manual*, *Eur. Phys. J.* **C 58** (2008) 639 [arXiv:0803.0883] [INSPIRE].

[5] G. Curci, W. Furmanski and R. Petronzio, *Evolution of Parton Densities Beyond Leading Order: The Nonsinglet Case*, *Nucl. Phys.* **B 175** (1980) 27 [INSPIRE].

[6] R.K. Ellis, H. Georgi, M. Machacek, H.D. Politzer and G.G. Ross, *Factorization and the Parton Model in QCD*, *Phys. Lett.* **B 78** (1978) 281 [INSPIRE].

[7] G. Heinrich, *Improved techniques to calculate two-loop anomalous dimensions in QCD*, Ph.D. thesis, Swiss Federal Institute of Technology, Zurich (1998). http://dx.doi.org/10.3929/ethz-a-001935934.

[8] S. Jadach, A. Kusina, M. Skrzypek and M. Slawinska, *Two real parton contributions to non-singlet kernels for exclusive QCD DGLAP evolution*, *JHEP* **08** (2011) 012 [arXiv:1102.5083] [INSPIRE].

[9] O. Gituliar, *Higher-Order Corrections in QCD Evolution Equations and Tools for Their Calculation*, arXiv:1403.6897 [INSPIRE].

[10] O. Gituliar, S. Jadach, A. Kusina and M. Skrzypek, *On regularizing the infrared singularities in QCD NLO splitting functions with the new Principal Value prescription*, *Phys. Lett.* **B 732** (2014) 218 [arXiv:1401.5087] [INSPIRE].

[11] M. Skrzypek, O. Gituliar, S. Jadach and A. Kusina, *The new PV prescription for IR singularities of NLO splitting functions*, PoS(LL2014)059 [arXiv:1407.6261] [INSPIRE].